

# Investigation and validation of wake model combinations for large wind farm modelling in neutral atmospheric boundary layers

**E Tromeur, S Puygrenier, S Sanquer**

Meteodyn France, 14bd Winston Churchill, 44100, Nantes, France

Email: eric.tromeur@meteodyn.com

**Abstract.** This study is focused on assessing the ability of two refined large wind farm models to describe the disturbance of the neutral atmospheric flow caused by large offshore wind farms. Sensitivity studies of internal boundary layer parameters are carried out. An optimum large wind farm correction is then proposed and combined with two different standard single wake models, the Park and EVM models. The large wind farm wake effect is evaluated and validated against measurements of two offshore wind farms at Horns Rev and Nysted and four standard wake models by computing velocity deficit and normalized power. All large wind farm models proposed were able to capture wake width to some degree and the decrease of power output moving through the wind farm. Despite some uncertainties, this very promising model combinations allows us to take into account the slowdown in large wind farms.

**Keywords:** wake model, atmospheric boundary layer, wind farm

## 1. Introduction

When air under neutral conditions flows from one surface through a wind turbine with a different roughness, the air is slowed [1] [2], reducing the wind velocity (Figure 1, left and side). The region in the flow behind the turbine is called the wake of a wind turbine. Its effects are seen as wake effects.

Generally, these effects can be neglected when the turbines are spaced apart by more than 10 rotor diameters. However, the turbines are increasingly clustered in large wind farms, the spacing between turbines being usually smaller because of the very favorable wind conditions on some sites. In that case, an internal boundary layer grows downwind from the roughness change [3][4][5] (Figure 1, right and side), the turbines influencing each other. A large wind farm wake effect then occurs by combination of single wake effects and this internal boundary layer modification (Figure 1).

Wake models in wind resource softwares like WindFarmer [6], ECN-Wakefarm [7], WAsP [8][9], NTUA [10] or Meteodyn WT [11] were evaluated for small wind farms [12] or single wakes [13]. However, it has become apparent that standard single wake models as Park [14][15] and EVM [16] models tend to underestimate wake losses in large wind farms as offshore arrays [17]. It is thus important to compute correctly the velocity deficit by taking into account the large wind farm wake effect.

Nowadays, two types of models are used to estimate velocity deficit and power losses due to wind turbine wakes. One is a wind farm model using a wake model that has been simplified or parameterized. The second is a CFD-type  $k-\epsilon$  model which solves basic equations of the atmosphere and produces results on a fine mesh in space and time [18]. In particular, Schlez and Neubert [6] described the disturbance of the atmospheric flow caused by the wind farm with an empirical large wind farm correction. However, there are uncertainties in their extrapolation which need to be further explored [6].



The goal of this paper is to assess the ability of two refined large wind farm models based on [6] to describe the disturbance of the neutral atmospheric flow caused by the wind farm. Sensitivity studies of internal boundary layer parameters are first carried out. An optimum large wind farm correction is then proposed and combined with two different standard single wake models, the Park [14][15] and EVM [16] models. The large wind farm wake effect is finally evaluated and validated against measurements of two offshore wind farms and four standard wake models as in [18] by computing velocity deficit and normalized power.

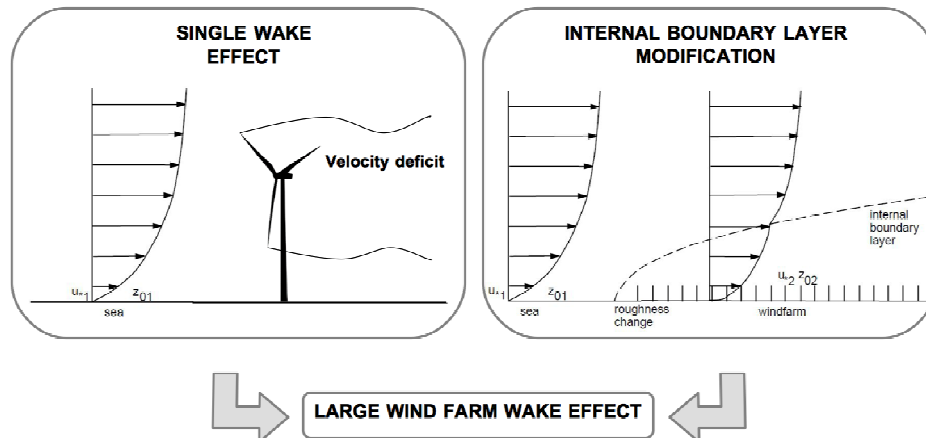


**Figure 1:** Sketch of large wind farm wake effect

## 2. Methodology

Single wake models don't consider the change of the atmospheric boundary layer by the additional roughness associated with wind turbines. More wind turbines are far from the windward side of the park, more the velocity deficit increases due to speed slowing down over the park. Therefore, the boundary layer profile is a function of the equivalent roughness  $z'_0$  and the wind position relative to the upstream turbine.

Three sensitivity studies are performed to optimize the large wind farm correction:

1. equivalent roughness  $z'_0$  computation
2. internal boundary layer profile estimation
3. large wind farm correction activation

The large wind farm correction is parametrized according to Horns Rev offshore wind farm data and validated against production data at Nysted offshore wind farm as in [18]. The velocity deficit is then calculated in each point of the wind farm by combining a single wake effect from a wind turbine with this boundary layer modification. Two different standard single wake models are considered: the Park model [14][15] and the fast algorithm for EVM model [19] implemented in Meteodyn WT software [11]. Thereafter, these two large wind farm models are named WT Park+IBL and WT Fast EVM+IBL.

A model intercomparison is finally performed at the two offshore wind farms. These two combined models are compared with four different wake models: WindFarmer [6], ECN-Wakefarm [7], WAsP [8][9] and NTUA [10] as in [18].

An overview of the main features of the models used in this intercomparison is given in [20]. Some of the models applied are industry standard models, for example, WAsP, WindFarmer, WT Park+IBL and WT Fast EVM+IBL, whereas others are primarily research models. In WAsP, the Park model is used as a wake model while a large wind farm correction is combined with this single wake model in the WT Park+IBL model.

Besides, both large wind farm models WT Fast EVM+IBL and WindFarmer are based on the same single wake model, namely the EVM model. However, the main differences are in the boundary layer modification parameterization which is the goal of this paper.

There are a number of issues in comparing model simulations and wind farm observations of velocity deficit and power losses in wakes that were detailed in [20]. It is difficult to make exactly the same simulations with models of different types even after the main variables, such as thrust coefficient, wind speed at hub height, free-stream wind profile, etc., have been set. Examples of this are that it is not possible to run WAsP for extremely narrow wind speed and direction bins because WAsP relies on a Weibull fit to the wind speed observations. For CFD, one issue is to accurately determine the turbulence profile and to recall that, for narrow sectors, the wake is centered on the given direction and no directional variability is included [18].

There are also practical issues relating to computing resources. Running a full wind farm simulation in WAsP or Meteodyn WT takes of the order of minutes, while in the NTUA model requires a time scale of days to make even one simulation limiting the number of runs performed.

To provide a quantitative evaluation of the refined large wind farm model performances versus the observations and other wake models, the normalized power and its root-mean-square-error (RMSE) are compared for each case.

This normalized power is defined in the next section presenting briefly the two offshore wind farms.

### 3. Measurements

The observations used to parameterize and validate the large wind farm correction are taken from the large offshore wind farms at Horns Rev [21] and Nysted [22][23] in Denmark. The turbine spacing at Horns Rev is  $7 D_{rotor}$  in both north–south and west–east directions (Figure 2), whereas at Nysted the turbine spacing is  $5.8 D_{rotor}$  in the north–south direction and  $10.5 D_{rotor}$  in the east–west direction (not shown).

To examine the single wake, the average power at each turbine is calculated in each column of the wind farm for seven wind direction sectors centered on an exact wind farm row (ER) ( $270^\circ \pm 2.5^\circ$  at Horns Rev and  $278^\circ \pm 2.5^\circ$  at Nysted), and for mean wind directions of  $+5^\circ$ ,  $+10^\circ$ , and  $+15^\circ$  and  $-5^\circ$ ,  $-10^\circ$ , and  $-15^\circ$  from ER. Flow down at ER thus represents the likely maximum wake effect, while the wind directions that are slightly offset from ER assist in assessing the wake width.

Finally, The power in each column is normalized to the power in the first column (1 ... 8 at Horns Rev). In both cases, wake effects is evaluated for a free-stream velocity mainly coming from the west (not shown) and equal to  $8 \text{ m.s}^{-1}$  as in [18].

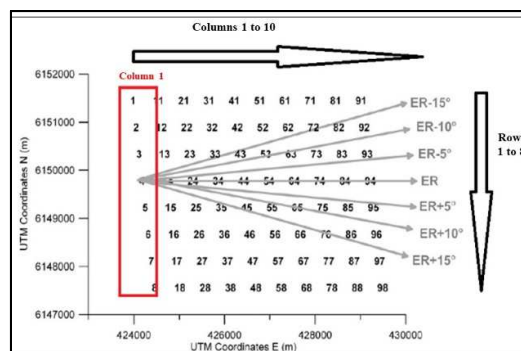


**Figure 2:** Horns rev wind farm layout [18].

## 4. Large wind farm wake effect: parametrization and activation

### 4.1. Roughness $z'_0$ influence

The equivalent roughness  $z'_0$  is calculated with the method of Frandsen [24][25] for each wind direction and wind speed at each turbine. It depends on the spacing between two rows of wind turbines along the wind direction  $S_d$  and the crosswind direction  $S_c$ .  $S_c$  has a huge influence on the roughness (example on Figure 3 for the wind turbine number 74 (WT74) at the Horns Rev with  $S_d = 7$ ). It impacts directly the velocity deficit coefficient correction and the normalized power with respect to WT04, the last one going down to 10% if  $S_c = 3$  and the wind speed is equal to  $8 \text{ m.s}^{-1}$  (not shown).

An algorithm is developed to calculate  $S_c$  and  $S_d$  whatever the type of wind farms and the wind directions. Figure 4 presents an example of  $S_c$  and  $S_d$  evolutions at Horns Rev for ER incidence (other incidences not shown here). The number of upstream wind turbines for a specific position is increasing for a wind turbine going far away from the first column of the array.  $S_c$  and  $S_d$  are homogeneous over the all wind farm considering at least one wind turbine is detected upstream. Finally,  $S_c$  and  $S_d$  has been found equal to 7 for both wind farms in Denmark.

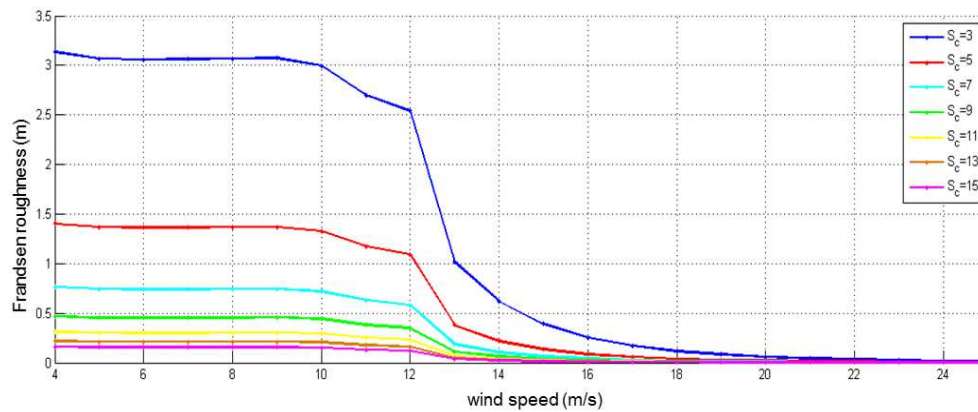


**Figure 3:** Frandsen roughness function of wind speed and  $S_c$  with  $S_d=7$  at ER incidence and wind turbine WT74

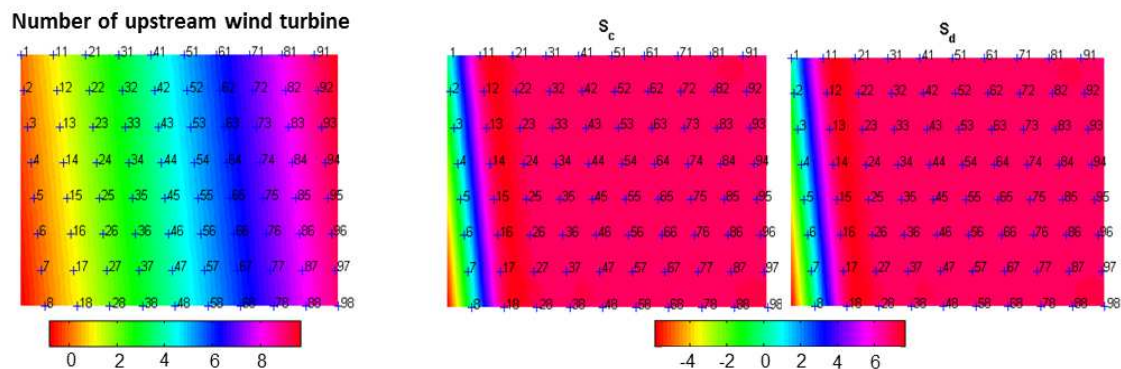


**Figure 4:** Evolution of  $S_c$  and  $S_d$  at ER incidence at Horns Rev

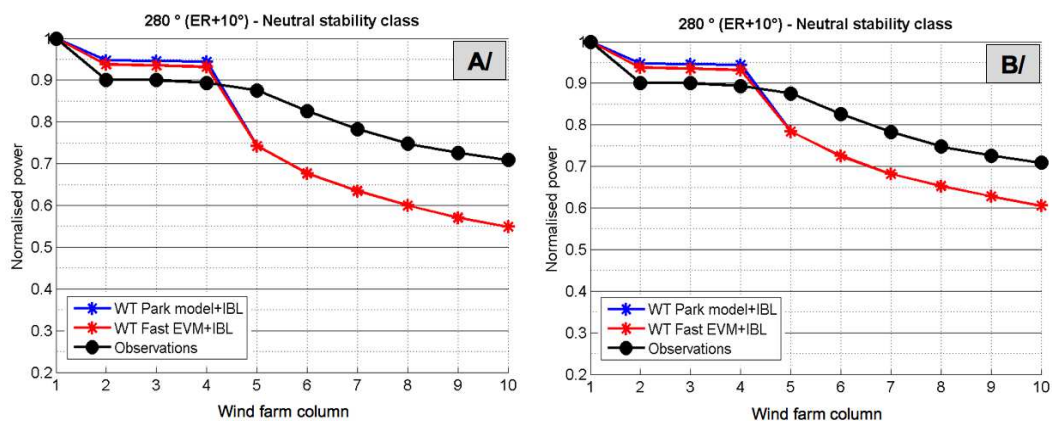


**Figure 5:** Normalized power at ER +15° at Horns Rev for  $h_{ibl} = 0.09h$  (A/) and  $h_{ibl} = 0.05h$  (B/).

#### 4.2 . Internal boundary layer influence

The velocity deficit coefficient correction is the ratio between the wind speed in the IBL and the wind speed taken at the same height before the roughness change. However, an offset  $H_{start}$  (function of the fetch and  $z'_{0.}$ ) from which the boundary layer starts and the IBL height  $h_{ibl}$  influence it. Sensitivity studies of  $H_{start}$  and  $h_{ibl}$  are then carried out at Horns Rev with the two combined wake models in order to optimize wind speed and power corrections:

- ◆ According to [26],  $0.05h \leq h_{ibl} \leq 0.09h$ , where  $h$  is the boundary layer height. Comparisons between both combined models and observations in Figure 5 show a better agreement for  $h_{ibl}=0.05h$  (case B/) against 9% of  $h$  in [6]. The same is observed for all other directions, except for ER-15° (not shown).
- ◆ As shown in Table 1, the more  $H_{start}$  is low, the more velocity and power deficits are low. On the contrary to [6] proposing  $H_{start} = 2/3 h_{hub}$  (with  $h_{hub}$  the hub height), the optimum  $H_{start}$  is equal to zero, meaning the inner boundary layer influence starts from the ground.

All these optimized parameters are considered by default in the next validation section 5.

**Table 1:** Evolution of wind speed and power correction function of  $H_{start}$  for the wind turbine WT74 at incidence ER at Horns Rev (WT Park+IBL model).  $D_{rotor}$  is the rotor diameter.

$H_{start}$	Coefficient Correction WT74	Power Correction WT74
0	0.83	0.57
1/4 $H_{hub}$	0.78	0.47
1/3 $H_{hub}$	0.76	0.45
$H_{hub}-D_{rotor}/2$	0.75	0.41
2/3 $H_{hub}$	0.66	0.27

#### 4.3 . Large wind farm correction activation

A geometric measure of turbine density is used to activate the large wind farm correction. For each small direction sector, the horizon is scanned and the presence of upstream turbines detected. On the contrary to [6], an optimum turbine density for 5° sectors is parameterized rather than 30° sector. Several angular sectors between 5° and 30° have been tested (not shown) to find this optimum sector. The large wind farm correction to ambient wind speed is then applied if there is at least one turbine in the selected sector.

Figure 6 shows a schematic diagram for wind turbine identification. Two wind turbines are in a sector  $[Dir-\alpha; Dir+\alpha]$  with  $Dir$  being the wind direction and  $\alpha$  the half turbine density sector. In that case, the large wind farm correction is combined to the single wake model to estimate the large wind farm wake effect. This model is always activated from the fourth wind farm column.

Finally, the velocity deficit is computed as the velocity deficit minimum taken between the large wind farm model and the single wake Park or Fast EVM models.

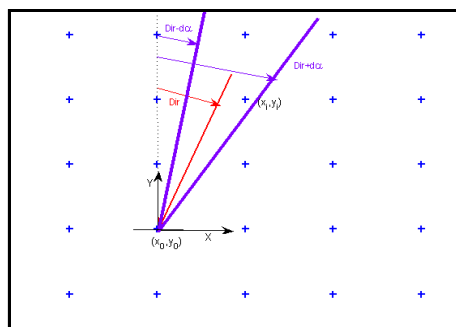


**Figure 6:** Schematic diagram for wind turbine identification



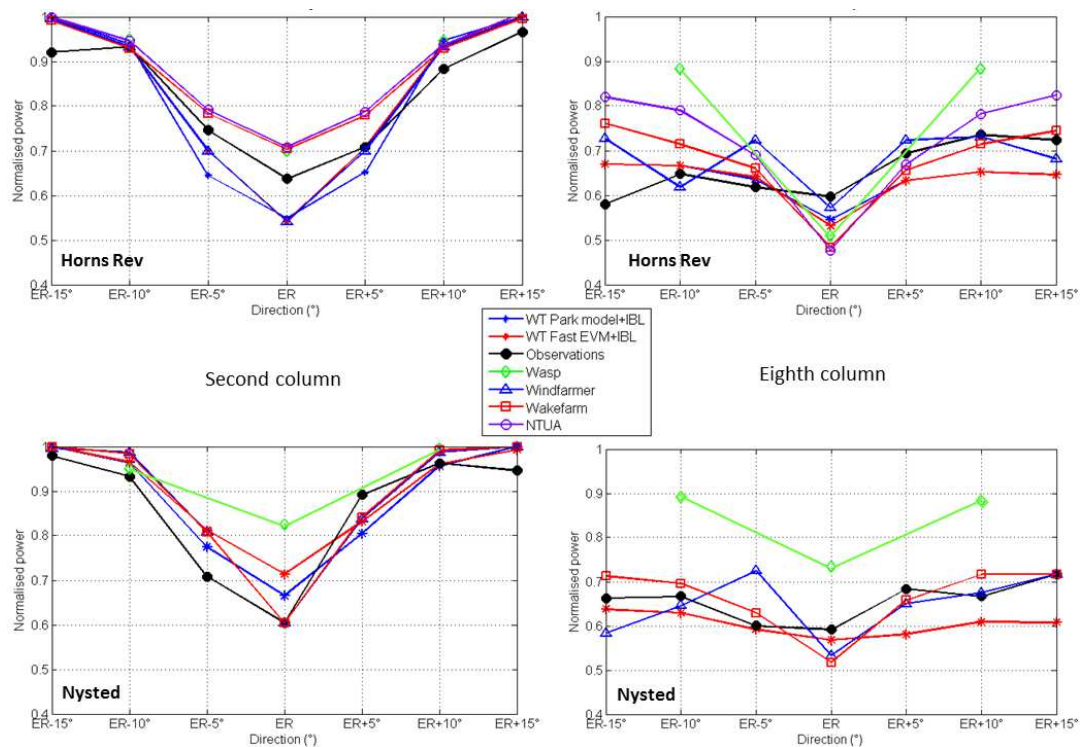


**Figure 7:** Mean normalized power from Horns Rev (top), Nysted (down) and model simulations for the second (left) and the eighth (right) columns of wind turbines.

## 5. Model comparisons with offshore wind farm data

A model intercomparison is performed at the two offshore wind farms for four different wake models as in [18] and the two combined models.

### 5.1. Wake width

As for other models, WT Park+IBL and Fast EVM model+IBL capture well the wake width at the second column of wind turbines (Figure 7) and show greater agreement with the observed wake depth than WAsP though both overestimate (respectively underestimate) the magnitude of the wake width at Horns Rev (Nysted).

For the entire wind farm (column 8), normalized powers of both combined models fit better with observations than other models even if they tend to overestimate (underestimate) the power for sectors less (greater) than ER.

In general, the root-mean-square error (RMSE) of normalized power shown in Table 2 indicates that WT Park+IBL and WT Fast EVM+IBL models perform better (i.e., exhibit lower RMSE) for direct flow down the row (i.e., ER) than for oblique angles.

### 5.2. Power deficit by downwind distance

Averaged normalized power as a function of downwind distance for a freestream wind speed of  $8 \text{ m.s}^{-1}$  for the seven wind directions are shown in Figure 8 (Horns Rev) and Figure 9 (Nysted). Both combined models appear to capture the shape of power deficit as a function of distance into both wind farms. In particular, this model has a very good agreement with observations at incident wind directions of ER-10°, ER-5°, ER+5° for Horns Rev and ER-15°, ER-10°, ER+10° for Nysted.

Moreover, WT Fast EMV+IBL model results have the same order of magnitude than data from Wakefarm and WindFarmer models, being even better at incident wind directions of 255°, 260°, 275° for Horns Rev and 263°, 268°, 273°, 288° for Nysted.

Overall the performance of a single wake model and the large wind farm correction combination is very promising.

**Table 2:** RMSE of normalized power from the models vs observations at Horns Rev (top) and Nysted (bottom).

Horns Rev						
Direction (°)	WT Park+IBL	WT Fast EVM+IBL	WindFarmer	Wakefarm	WAsP	NTUA
ER-15°	0.11	0.11	0.15	0.17		0.07
ER-10°	0.04	0.03	0.05	0.07	0.17	0.11
ER-5°	0.05	0.03	0.05	0.03		0.03
ER	0.06	0.06	0.04	0.08	0.06	0.08
ER+5°	0.07	0.05	0.04	0.05		0.04
ER+10°	0.08	0.08	0.03	0.03	0.11	0.03
ER+15°	0.07	0.07	0.07	0.03		0.10

Nysted					
Direction (°)	WT Park+IBL	WT Fast EVM+IBL	WindFarmer	Wakefarm	WAsP
ER-15°	0.02	0.02	0.09	0.05	
ER-10°	0.04	0.04	0.05	0.04	0.21
ER-5°	0.04	0.06	0.13	0.10	
ER	0.04	0.07	0.04	0.06	0.09
ER+5°	0.08	0.07	0.04	0.03	
ER+10°	0.03	0.03	0.04	0.03	0.12
ER+15°	0.07	0.06	0.03	0.04	

## 6. Discussion and conclusion

A new correction to the classic wind farm wake model is presented that allows the disturbance of the ambient flow field caused by large wind farms to be modelled. Sensitivity studies of internal boundary layer parameters are carried out in order to assess the combination of single wake models (Park or Fast EVM) with a refined version of boundary layer model based on [6] and [26].

The two new combined model simulations were evaluated comparing wake width and normalized power output by turbine moving through the wind farm. The large wind farm models were able to capture wake width to some degree and the decrease of power output moving through the wind farm. Root-mean-square errors indicate generally better model performance for direct down the row flow than for oblique angles.

The large wind farm correction compared with four standard wake models is then validated with success for two offshore wind farms (Horns Rev and Nysted), solving a complex flow problem with little computational cost. This suggests that both combined wake models proposed assess well the power losses in those wind farms.

The main strength of this new correction is the automatic estimation of the spacing between two rows of wind turbines along the wind direction  $S_d$  and the crosswind direction  $S_c$ . Indeed, the new algorithm developed to calculate  $S_c$  and  $S_d$  allows us to estimate directly the equivalent roughness  $z'_0$  for each wind direction and wind speed at each turbine whatever the type of wind farms.

However given the limited set of validation cases there is still uncertainties in such extrapolation. The large wind farm model based on fundamental physics of the boundary layer is designed to scale to offshore wind farm layouts. In particular, the internal boundary layer parametrization depends on these wind farms and their equivalent roughness  $z_0$ .

Further validation cases are then needed and the large wind farm correction should be also tested on onshore wind farms where the topography is more complex.

In the future, a linear combination of single wake models with the boundary layer modification will be assessed to compute velocity and power deficits. Moreover, the influence of thermal stratification of the boundary layer will be also evaluated.

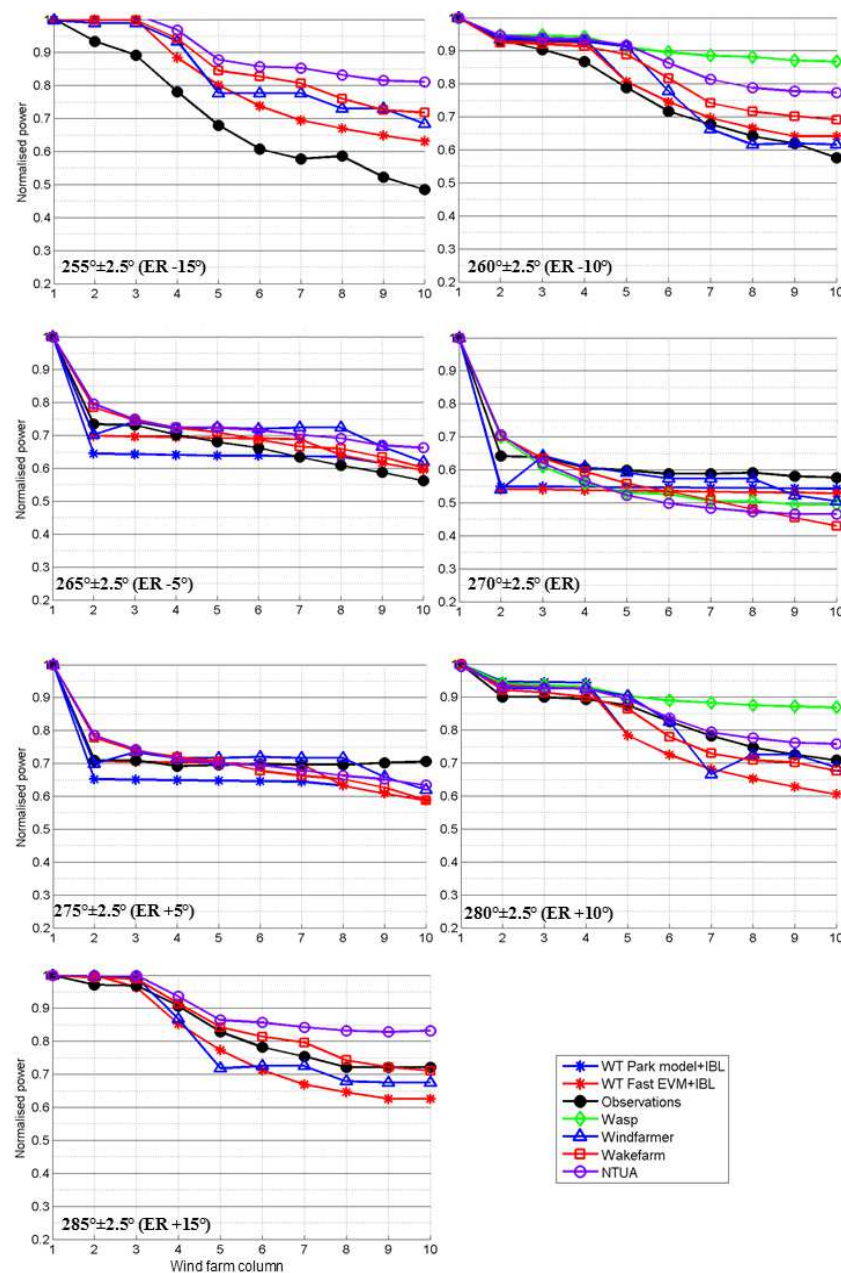


**Figure 8:** Normalized power at Horns Rev.



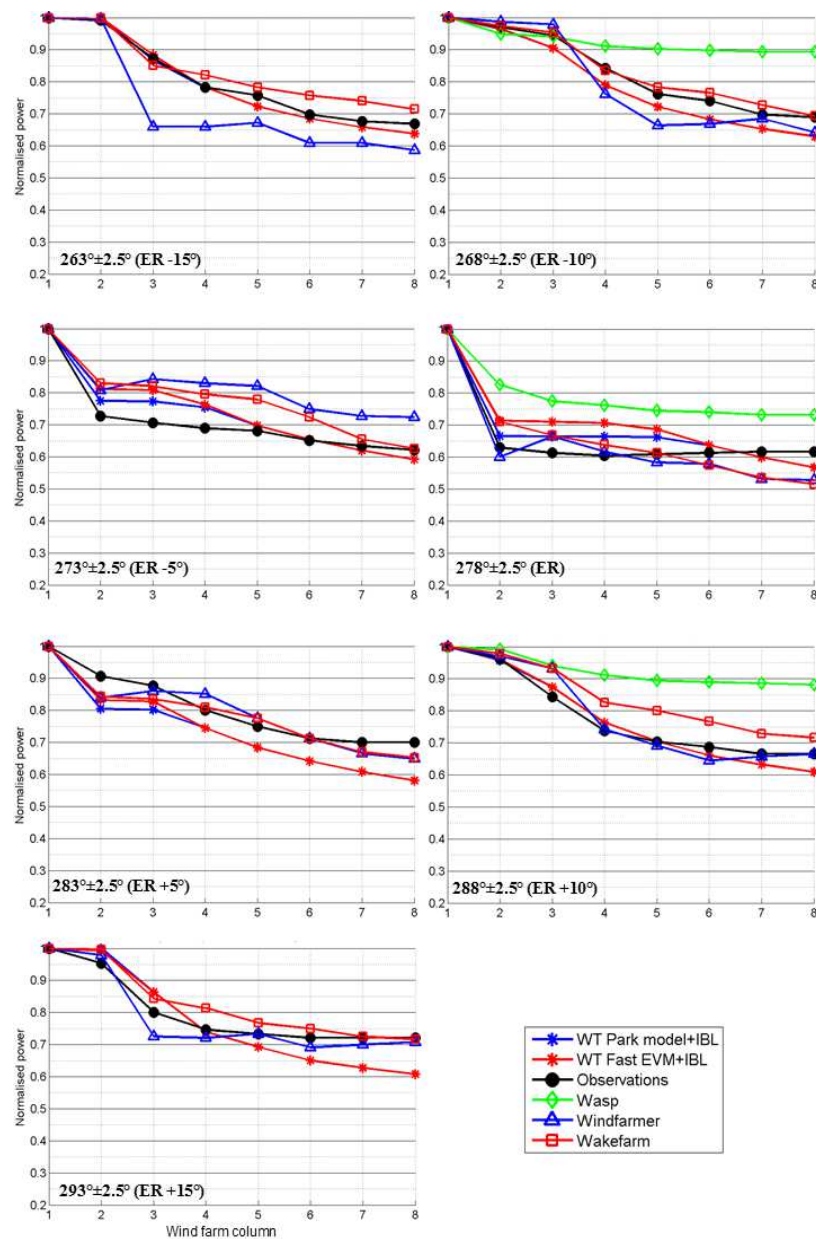


**Figure 9:** Normalized power at Nysted.

### Nomenclature

$da$	Half turbine density sector ( $^{\circ}$ )
Dir	Wind direction ( $^{\circ}$ )
$D_{rotor}$	Rotor diameter ( $m$ )
$\varepsilon$	Turbulent dissipation rate ( $J/(kg.s)$ )
ER	Exact wind farm row ( $^{\circ}$ )
$h$	Boundary layer height ( $m$ )
$h_{hub}$	Hub height ( $m$ )
$h_{ibl}$	Internal boundary layer height ( $m$ )
$H_{start}$	Boundary layer offset ( $m$ )
$k$	Turbulent kinetic energy ( $m^2.s^{-2}$ )
$S_c$	Spacing between two wind turbine rows along the crosswind direction( $m$ )
$S_d$	Spacing between two wind turbine rows along the wind direction ( $m$ )
$z'_0$	Equivalent roughness ( $m$ )

### Acronyms

CFD	Computational Fluid Dynamics
ECN	Energy research Center of the Netherlands
EVM	Eddy Viscosity Model
IBL	Internal Boundary layer
NTUA	The National Technical University of Athens
RMSE	Root-mean-square error
WasP	Wind Atlas Analysis and Application Program

## References

- [1] Crespo A, Hernandez J, Frandsen S. "Survey of modelling methods for wind turbine wakes and wind farms". *Wind Energy* 1999; 2:1-24.
- [2] Vermeer LJ, Sørensen JN, Crespo A. "Wind turbine wake aerodynamics". *Progress in Aerospace Sciences* 2003; 39:467-510.
- [3] Bradley EF. "A micrometeorological study of velocity profiles and surface drag in the region modified by a change in surface roughness". *Quart. J. R. Met. Soc.* 1968; **94**:361-379.
- [4] Jensen NO. "Change of surface roughness and the planetary boundary layer", *Quart. J. R. Met. Soc.* 1978; 104:351-356.
- [5] Rao KS., Wyngaard JC, Coté DR. "The structure of the two-dimensional internal boundary layer over a sudden change of surface roughness". *J. Atmos. Sci.*, **26**, pp. 432-440, 1974.
- [6] Schlez W, Neubert A. "New developments in large wind farm modelling". *Proc. European Wind Energy Conf.*, Marseille, France, 2009; EWEA PO.167, 8 p.
- [7] Schepers, JG. "ENDOW: Validation and improvement of ECN's wake model". *Energy Research Center for the Netherlands rep.* ECN-C-03-034, 2003; 113 p.
- [8] Mortensen NG, Heathfield DN., Myllerup L, Landberg L, Rathmann O. "Wind atlas analysis and application program: WASP 8 help facility". *Risø National Laboratory*, Roskilde, Denmark, 2005.
- [9] Rathmann O., Barthelmie RJ, Frandsen ST. "Turbine wake model for wind resource software". *Proc. European Wind Energy Conf.*, Athens, Greece, EWEA 2006, BL3.313.
- [10] Magnusson M., Rados KG, Voutsinas SG. "A study of the flow downstream of a wind turbine using measurements and simulations". *Wind Eng.* 1996; 20:389-403.
- [11] Li R., Delaunay D, Jiang Z. "A new Turbulence Model for the Stable Boundary Layer with Application to CFD in Wind Resource Assessment". *EWEA Proceedings*, Paris, France, 17-20 November, 2015; 9 p.
- [12] Barthelmie RJ and Coauthors. "Efficient development of offshore windfarms (ENDOW): Modelling wake and boundary layer interactions". *Wind Energy* 2004; 7, 225-245.
- [13] Barthelmie RJ, Folkerts L, Rados K, Larsen GC, Pryor SC, Frandsen S, Lange B, Schepers G. "Comparison of wake model simulations with offshore wind turbine wake profiles measured by sodar". *J. Atmos. Oceanic Technol.* 2006; 23, 88-901.
- [14] Jensen NO. "A note on wind generator interaction". *Technical report from the Risø National Laboratory (Risø-M-2411)*, Roskilde, Denmark, 1983; 16 p.
- [15] Katic I, Højstrup J, Jensen NO. "A simple model for cluster efficiency". *EWEA Proceedings*, Rome, Italy, 1986; 5 p.
- [16] Ainslie JF. "Calculating the flowfield in the wake of wind turbines". *I. Wind Eng. And Ind Aero.*, 1988; 27:213-224.
- [17] Beaucage P, Robinson N, Brower M, Alonge C. "Overview of six commercial and research wake models for large offshore wind farms". *EWEA Proceedings*, Copenhagen, Germany, 16-19 April, 2012; 10 p.
- [18] Barthelmie RJ, Pryor SC, Frandsen ST, Hansen KS, Schepers JG, Rados K, Schlez W, Neubert A, Jensen LE, Neckelmann S. "Quantifying the Impact of Wind Turbines Wakes on Power Output at Offshore Wind Farms". *Journal of Atmospheric and Oceanic Technology*, 2010; 27: 1302-1317.
- [19] Anderson M. "Simplified solution to the Eddy-Viscosity wake model". RES document 01327-202, Issue 02, 10 July 2009.
- [20] Barthelmie RJ, and Coauthors. "Modelling and measuring flow and wind turbine wakes in large wind farms offshore". *Wind Energy*, 2009, 12, 431-444, doi:10.1002/we.348.
- [21] Jensen, L. "Wake measurements from the Horns Rev wind farm. Proc". European Wind Energy Conf., London, United Kingdom, European Wind Energy Association, 2004.
- [22] Barthelmie RJ, Rethore, P. E. and Jensen L. "Analysis of atmospheric impacts on the development of wind turbine wakes at the Nysted wind farm". Proc. European Offshore Wind Conf., Berlin, Germany, European Wind Energy Association, PO.36., 2007c [Available online at [http://www.eow2007proceedings.info/allfiles2/132\\_Eow2007fullpaper.pdf](http://www.eow2007proceedings.info/allfiles2/132_Eow2007fullpaper.pdf).]
- [23] Cleve, J., M. Grenier, P. Enevoldsen, B. Birkemose, and L. Jensen. "Model-based analysis of wake-flow data in the Nysted off-shore wind farm". *Wind Energy*, 2009, 12, 125-135, doi:10.1002/we.314.
- [24] Frandsen S, Barthelmie R, Pryor S, Rathmann O, Larsen S, Højstrup J, Thøgersen M. "Analytical modelling of wind speed deficit in large offshore wind farms". *Wind Energy*, 9, 2006.
- [25] Frandsen ST. "Turbulence and Turbulence-Generated Structural Loading in Wind Turbine Clusters". *Technical report from the Risø National Laboratory (Risø-R-1188)*, Roskilde, Denmark, 2007; 130p.
- [26] Larsen S, Mortensen E, Gylling N, Sempreviva AM, Troen, Ib. "Response of neutral boundary layers to changes of roughness". *Meteorology and Wind Energy Department. Annual Progress Report*. 1 January - 31 December 1987; pp. 15-43.